processes

MDPI

Article

Design and Modelling of Heat-Coupled Storage System with High- and Low-Pressure Bypass: Electrothermal Characteristics and Peak Regulating Performance

Han Yang, Sun Tao and Ma Honghe *

School of Electrical and Power Engineering, Taiyuan University of Technology, Taiyuan 030024, China
* Correspondence: mahonghe@tyut.edu.cn

Abstract: To achieve a balance between supply and demand during cogeneration system operation, it is necessary to improve the peak regulation capacity and regulatory flexibility of the unit. Considering the excellent performance of energy storage systems, a heat-coupled storage system with high- and low-pressure bypass is proposed to increase peak regulation capacity. Employing a 300 MW heating unit as the research object, thermal system models of a traditional-pumping steam-heating system, a high- and low-pressure bypass heating system, and a coupled system were built using Aspen Plus software. The electric heating characteristics of the three systems, as well as the peak regulation capacity and peak regulation depth of the coupled system, were analysed under different storage and heat release loads. Results indicate that the high- and low-voltage bypass system and the coupled system both improve the peak capacity and control flexibility of the unit. Moreover, the coupled system has a greater influence on the maximum thermoelectric ratio and minimum charge rate than the high- and low-voltage bypass heating system, thereby extending the range of safe operation. The peak capacity and depth of heat storage are 65.55 MW and 21.85%, respectively, while the peak capacity and the depth of the heat-release process are 39.32 MW and 13.10%.

Keywords: heat-coupled storage system; high- and low-pressure bypass; peak regulation; Aspen Plus

Citation: Yang, H.; Tao, S.; Honghe, M. Design and Modelling of Heat-Coupled Storage System with High- and Low-Pressure Bypass: Electrothermal Characteristics and Peak Regulating Performance. *Processes* **2023**, *11*, 1104. https://doi.org/10.3390/pr11041104

Academic Editor: Davide Papurello

Received: 27 February 2023
Revised: 25 March 2023
Accepted: 27 March 2023
Published: 4 April 2023

1. Introduction

To reach the development goal of "peak carbon by 2030 and carbon neutrality by 2060", the installed capacity of renewable energy generation is expanding every year. Due to the intermittent and unpredictable nature of renewable energy generation, thermal power plants are essential for increasing peaking capacity and flexibility in regulation [1]. The application of thermoelectric coupling technology has solved this problem since units can be retrofitted to meet both the heating demand and peaking capacity of the unit [2]. High- and low-pressure bypass heating [3], low-pressure cylinder no-load heating [4], heat storage [5], absorption heat pumps [6], and electrode boilers [7] are the primary technologies of thermoelectrolytic coupling transformation [8].

In recent years, numerous studies concerning high- and low-pressure bypass-heat supply and storage tanks have been conducted. Xue et al. [9] studied the impact of high- and low-pressure bypass heating on unit-heating capacity. The findings revealed that retrofitting deep peaking and high- and low-pressure bypass heating had a limited impact on the heating capacity of the unit. Wang et al. [10] established a mathematical model based on bypass heating and proposed an operating strategy according to the actual grid peaking needs of the unit. The results indicated that the traditional heat-supply method of steam extraction and the high- and low-pressure bypass switching could improve the renewable-energy consumption capacity of the unit by 324.46%. Liu et al. [11] established a thermodynamic analytical model of thermoelectric coupling technology to quantitatively analyse a 350 MW combined heat and power (CHP) unit. It was found that thermoelectrolytic coupling technology extended the feasible operating range of the system

and reduced the minimum electrical load, suggesting that heat-storage-tank decoupling technology was a preferable energy-saving option. Wang et al. [12] modelled the thermal system of the unit and investigated the effect of the thermal storage tank capacity on the peaking range. The research findings demonstrated that the peaking range of the unit could be increased after performing the heat-storage tank modification. However, there was an upper limit to the increase in peaking range, which was restricted by the capacity of the heat-storage tank. Lai et al. [13] utilized heat extraction and storage as a means to reduce the generation load of a unit and provide room for additional new energy sources to be integrated into the grid. The hot-water storage tank was capable of balancing some of the unit-load requirements for the grid. Li et al. [14] used phase-change heat storage to store the energy of excess steam by modifying the original unit and then releasing the energy stored in the phase change through heat exchange to the unit's steam system to increase the unit's electrical load output when required. Trojan et al. [15] stored the pressure water from a deaerator in a hot-water storage tank without changing the boiler output load, thereby increasing the turbine pumping and reducing the electrical output of the turbine. During the heat-release phase, the water in the hot-water tank is introduced into the deaerator, thereby reducing the turbine draw and increasing the electrical output of the turbine. To improve the unit-heating capacity and increase the cogeneration unit wind-power consumption capacity, Liu et al. [16] established a mathematical model for wind-power consumption and used a combination of high- and low-pressure bypass heating and conventional steam extraction heating. Wang et al. [17] proposed a control principle to adapt the high-pressure bypass and low-pressure bypass flow rates to the characteristics of the high- and low-pressure bypass heating retrofit, which is of some significance for the smooth operation of the unit and the improvement of the parameters of the heating steam. The proposed control principle can further reduce the waste of steam with high parameters. These studies have achieved several enhancements, but there remain shortcomings in the comparative analysis of the electrothermal characteristics, maximum thermoelectric ratio, and minimum electrical-load factor of the unit after high- and low-pressure bypass heating transformation and coupled heat storage. Thus, further studies regarding peaking capacity and peaking depth are necessary.

In this paper, a 300 MW heating unit is employed as an example. Aspen Plus software is used to model the conventional extracted-heat supply system, high- and low-pressure bypass-heat supply system, and high- and low-pressure bypass-heat supply system coupled with a heat-storage tank. Three heat storage and release schemes were designed to align with the principle of graded energy utilization, avoiding the use of high- and low-pressure bypasses for direct-steam extraction, so that the design principle is consistent with the use of capacity ladders. Three heat storage and release schemes were designed to align with the capacity ladder principle, thereby avoiding the need for high- and low-pressure bypasses for direct-steam heating. Further analysis of the three schemes revealed that they have a lower electrical-load output for the same heating compliance and higher heating compliance for the same electrical-load output. This enhances the peaking capacity of the thermal-power unit, improves its heating capacity, and provides a reference solution for the flexible modification of thermal-power units to use new energy generation as a peaking energy source. In contrast to traditional methods, such as steam extraction from the medium-pressure cylinder for heating and high- and low-pressure bypasses for heating, the designed schemes offer an alternative approach to consuming new energy generation.

2. Coupled Heat Storage System Unit Design

In response, the use of a high- and low-pressure bypass system for direct desuperheating and depressurization of steam for heating does not align with the principle of stepped energy utilization. To avoid energy waste caused by direct desuperheating and depressurization of high-parameter steam for heating, a heat-storage system coupled with a high- and low-pressure bypass system was chosen. The heat storage and release strategy for the coupled system involves applying the high- and low-pressure bypass-coupled heat

storage tank system. This approach decreases the load when the electric-load output of the unit needs to be reduced in the low-power consumption valley. THA (turbine heat acceptance) refers to the rated operating condition of a unit where the turbine is able to continuously operate and generate the rated power output with the rated steam inlet parameters, rated back pressure, normal commissioning of the heat-return system, and a 0% make-up water rate. When the electrical load of the heating unit is 40% THA, which is the minimum stable combustion load of the boiler, the high- and low-pressure cylinder bypass coupled-heat storage-tank system ceases to reduce the boiler load. At peak electricity consumption, the thermal-storage system releases heat in THA conditions to increase the electrical-load output of the unit. Referring to Zhang [18] et al., this work incorporated the storage and release capacities of the heat-storage tank, which were 30 MW, 60 MW, and 90 MW, respectively, in the heat-storage process design. The simulation in Aspen Plus software demonstrated that the storage and release capacities met the cycle requirements.

As Table 1 indicates, high- and low-pressure bypasses for direct desuperheating and depressurisation of reheated steam for heating do not align with the principle of graded energy utilization. The following three heat storage and release systems were designed for storage of the directly desuperheated and depressurised steam using molten salt, which can be used to increase the electrical-load output of the unit when the demand for electrical output increases. Three coupling methods with high- and low-pressure bypass heating are designed.

Table 1. Unit coupling system scheme.

Heat Storage Medium	Coupling Mode	Heat Storage Process	Exothermic Process
Ternary molten salt	R1	Heat resteam → deaerator	Feed-pump-outlet water → LP1 inlet steam
	R2	Heat resteam → deaerator	Feed-pump-outlet water → boiler-feed water
	R3	Cold resteam → deaerator	Feed-pump-outlet water → boiler-feed water

For R1, the heat-storage process involves heating the molten salt with steam taken from the reheater outlet, and the hydrophobic water, after heat exchange with the molten salt, enters the deaerator. This method avoids the use of low-pressure bypasses for direct-heat reduction and depressurization of the reheater outlet and inlet steam, which is not in line with the principle of graded energy utilization. In the heat-release process, the heated feedwater from the feed pump is heated to LP1 inlet parameters and enters LP1 to generate work for the turbine, directly increasing the electric-load output.

For R2, the heat storage process involves utilizing steam from the outlet of the reheater as the heat source to heat the molten salt and then exchange heat with hydrophobic water before entering the deaerator to avoid the use of a low-pressure bypass for direct heating. This approach is in accordance with the graded use of energy, which aims to avoid reducing the temperature and pressure of steam at the outlet and inlet of the reheater for direct heating. The heat-release process involves heating the molten salt with feed-pump-outlet water to reach the boiler-inlet feedwater temperature, resulting in the reduction of heat pumping steam from the high-pressure cylinder and medium-pressure cylinder. As a result, more high-temperature and high-pressure steam enters the turbine to generate more electrical output.

For R3, during the heat storage process, the molten salt is heated using steam at the inlet of the reheater, and the hydrophobic water is then exchanged with the molten salt before entering the deaerator. This helps to avoid the low-pressure bypass, which reduces the temperature and pressure of the steam at the reheater outlet and inlet and is not in line with the graded use of energy. During the heat-release process, the molten salt is heated using the feed-pump-outlet water, which is then heated to the boiler inlet feedwater temperature. This process reduces the amount of steam required for back-heat pumping in the high-pressure cylinder and medium-pressure cylinder, allowing more high-

temperature and high-pressure steam to enter the turbine and do work, thereby increasing the electric-load output.

Heat-storage tank size: cold tank 11.6 m diameter, 7.8 m high, hot tank 11.6 m diameter, 8.4 m high; heat storage material: cold tank ASTM A516-70 carbon steel, hot tank 304 stainless steel; specific heat of energy storage unit: 0.34 kcal/kg. The heat storage medium of the double-tank molten-salt storage tank is selected as ternary molten salt (53% potassium nitrate + 40% sodium nitrite + 7% sodium nitrate). Energy storage unit melt heat: 18 K cal/kg; the average thermal conductivity of the energy storage unit: 0.317 [19,20]. The focus of this study is on heat storage and release power, and, therefore, the size and material of the storage tank in the references were adequate in meeting the maximum heat storage and release power of 60 MW. In Figure 1, orange denotes the flow direction of the extracted high-temperature heat source, purple represents the flow of the extracted low-temperature heat source, while red and green symbolise the flow of the molten salt in the high- and low-temperature molten-salt tanks, respectively [21].

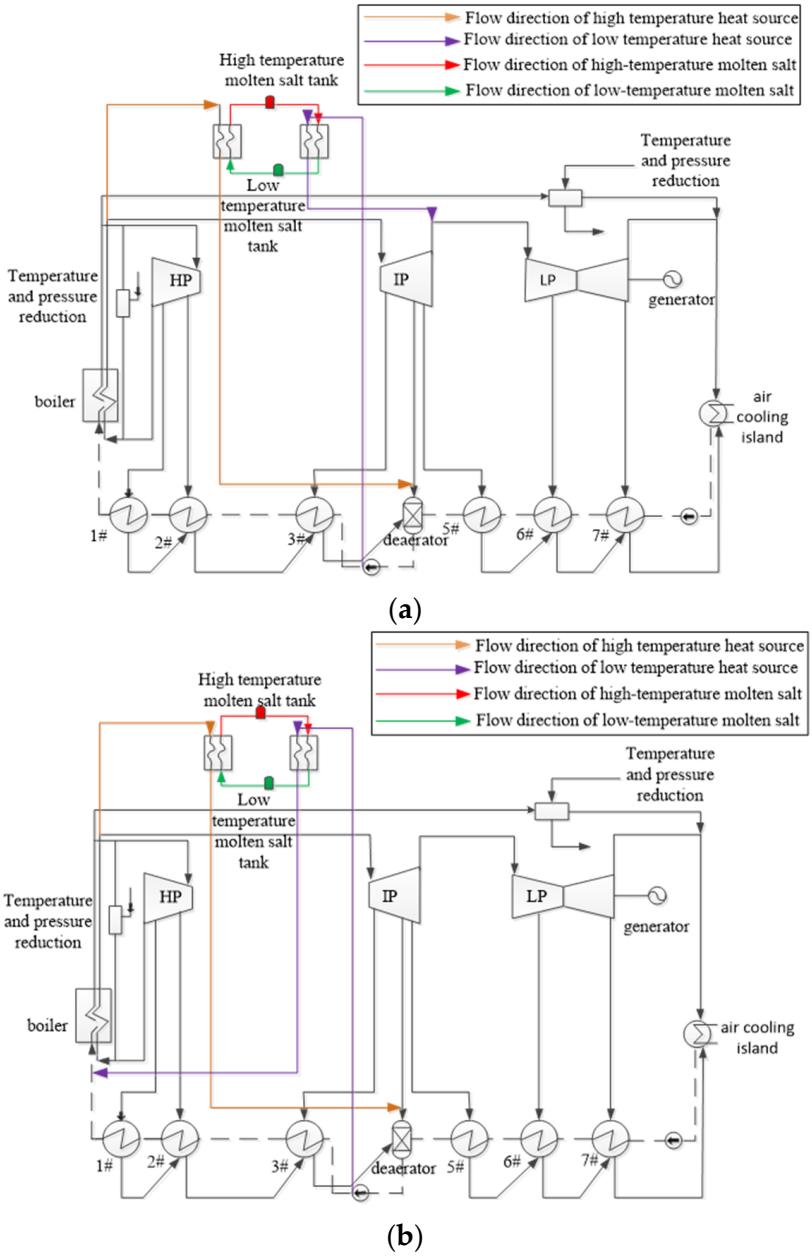

Figure 1. *Cont.*

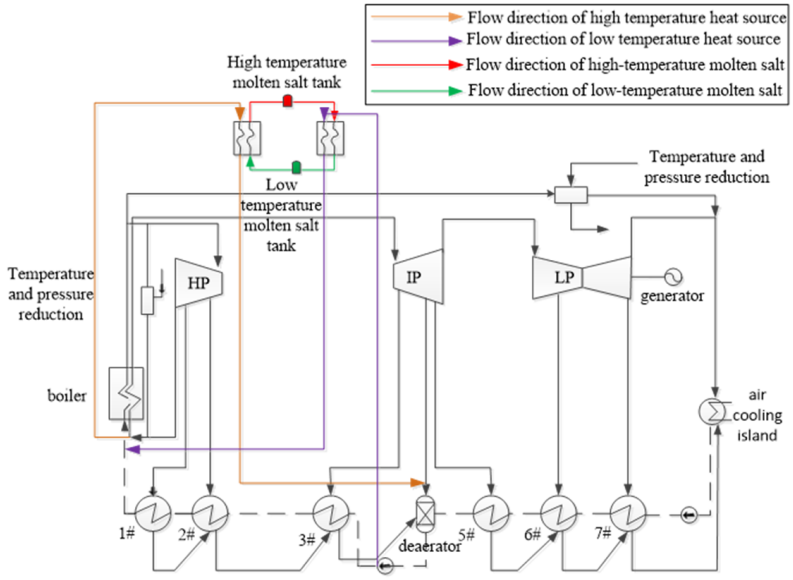

(**c**)

Figure 1. Unit-coupled heat-storage systems. (**a**) R1; (**b**) R2; (**c**) R3.

3. Model Building and Methodology

3.1. Modelling

In this paper, a 300 MW subcritical coal-fired direct air-cooled unit is used as the research object. The turbine is a two-cylinder, two-exhaust unit with one intermediate reheat and a rated back pressure of 14 kPa. Further, in addition to the fact that the 300 MW units are widely studied, the primary reason for choosing them as the focus of this work is that the foundation of this study is based on a 300 MW engineering example. As such, the parameters in this paper were based on the parameters of the 300 MW example unit. Although varying the values of heating units does open up more possibilities, due to the practicalities of this study, a 300 MW unit was selected as the subject. Exploring and analysing the heating-unit values in greater detail could be a promising avenue for future research. The selection of turbine parameters for this work is similar to the study by Li et al. [22]. The turbine parameters are listed in Table 2.

Table 2. Turbine parameters.

Parameters	Value
Rated main steam pressure/MPa	16.70
Rated main steam temperature/°C	538.0
Rated main steam capacity/t·h^{-1}	914.39
Rated reheat steam pressure/MPa	3.074
Rated reheat steam temperature/°C	538
Rated reheat steam capacity/t·h^{-1}	768.85
Rated back pressure/kPa	14
Rated feed water temperature/°C	268.4

The thermal system of the unit was modelled using Aspen Plus software [12]. The "Heater" model was applied in the heater to simulate the boiler, reheater, and air-cooled island. Moreover, the "Turbine Compr" model simulated the high-pressure, medium-pressure, and low-pressure cylinders. Also, the "HeatX" model of the two-strand logistics heat exchanger simulated the high-pressure heater and low-pressure heater, while the "Hopper" model was applied in the mixer to simulate the deaerator. The modules were connected through the material strands and after the process was built the STEAM-TA physical-property method was selected for the global setting. This approach enabled

calculations in a temperature range from 273.15 K to 1073 K and was applied to the constructed model.

3.2. Model Validation

To verify the accuracy of the numerical simulation, refer to the verification method of Li [15] et al. The simulated turbine-output values for the four operating conditions of THA, 75% slip pressure, 50% slip pressure, and 40% slip pressure of the unit were compared with the design values. As Table 3 indicates, the deviations between the simulated and design values were less than 5%, thereby meeting engineering simulation accuracy requirements and verifying that the model effectively simulates the variable working conditions of the unit [3].

Table 3. Comparison of steam engine thermal parameters under typical working conditions.

Condition	Design Value/MW	Simulation Value/MW	Relative Error/%
THA condition	300	287.88	4.04
Sliding pressure 75%	225	215.65	4.16
Sliding pressure 50%	150	145.62	2.92
Sliding pressure 40%	120	117.61	2.00

3.3. Minimum-Cooling Flow Rate

The minimum-cooling flow rate of the low-pressure cylinder is an important condition to ensure the safe operation of the low-pressure cylinder of the steam turbine. In order to ensure the safe operation of the steam turbine, the cooling flow rate of low-pressure cylinders must be safe. The cooling flow rate for low-pressure cylinders [23] can be calculated using Equations (1) and (2):

$$V_{min} = \frac{D_{c0} \times V_{c0}}{3.6} G_{v2min} \tag{1}$$

$$G_{cmin} = \frac{V_{min}}{v_c} \times 3.6 \tag{2}$$

where D_{C0} is the exhaust flow rate of the low-pressure cylinder under THA conditions, in t/h; V_{c0} represents the rated exhaust steam-specific capacity, in m^3/kg; V_{min} denotes the minimum volume flow of the final stage; G_{v2min} signifies the relative minimum volume flow of the final stage and is assumed to be 0.4; G_{cmin} is the minimum cooling flow of the low-pressure cylinder, in t/h; v_c denotes the exhaust steam-specific capacity of the low-pressure cylinder at different back pressures, in m^3/kg.

3.4. Thermoelectric Decoupling Performance Evaluation Index

The thermoelectric ratio and charge-rate indicators that evaluate the thermoelectric decoupling capability of the system are important indicators of the relationship between the unit-heating capacity and power-generation capacity.

The thermoelectric ratio [24] can be calculated using Equation (3):

$$x = \frac{Q_h}{P_e} \tag{3}$$

where P_e represents the output electrical load of the unit, in MW; Q_h denotes the thermal load of the unit, in MW.

The lowest charge rate is determined using Equation (4):

$$\lambda = \frac{P_e}{P_{e0}} \tag{4}$$

where P_e signifies the output electrical load of the unit, in MW; P_{e0} stands for the output electrical load of the unit under rated working conditions, in MW.

3.5. Performance Evaluation Index of the Coupling System

The newly added peak regulating capacity and peak regulating depth of the coupling system are indexes that evaluate the peak regulating the performance of the unit. It can reflect the proportional relationship between the output power load of the coupled system and the output power load of the uncoupled heat storage and release system. It can also intuitively reflect the peaking capacity of the unit. The heat storage and release processes are determined as follows [18]:

Heat-storage process:

$$\Delta P_{c,t} = P_0 - P_{c,t} \tag{5}$$

$$\Psi_{c,t} = \frac{\Delta P_{c,t}}{P_e} \tag{6}$$

Heat-release process:

$$\Delta P_{s,t} = P_{s,t} - P_e \tag{7}$$

$$\Psi_{s,t} = \frac{\Delta P_{s,t}}{P_e} \times 100\% \tag{8}$$

where $\Delta P_{c,t}$ and $\Delta P_{s,t}$ are the newly added peak-regulating capacity of time storage and heat-release process units, respectively, in MW; $\Psi_{c,t}$ respectively denote the peak regulating depth of time t storage and heat-release process units; $\Psi_{s,t} P_{c,t} P_{s,t}$ signify the output electrical load of the unit at time t of heat storage and heat release, in MW; P_0 and P_e, respectively, represent the output electrical load of the unit under the 40% THA and THA condition in MW.

4. Results and Analysis

4.1. Analysis of Electric Heating Characteristics

According to the simulations of the traditional extraction steam-heating system, the high- and low-pressure bypass heating system, and the coupled system built with Aspen In addition, the minimum cooling flow of the low-pressure cylinder and the regenerative extraction steam are satisfied. Figure 2 illustrates that when the maximum power of the heat-storage system and heat release is 60 MW, the output heat load and the electrical load of the unit can be obtained.

The electric heating characteristics of the R1, R2, and R3 schemes are shown in Figure 2a–c. Line AB represents the maximum-output load line of the boiler, BC shows the minimum cooling-flow load line of the low-pressure cylinder, and DC is the minimum-output load line of the boiler. Additionally, point B is the maximum heating load of the unit and the corresponding electrical load, while A and D, respectively, signify the maximum and minimum electrical load in the unit at the pure condensation condition. When the unit is under a certain thermal-load condition, the electrical load has a specific range of adjustability. M-N-B-L-H-I-F-D and J-K-B-L-H-I-F-D are the safe operating areas of the three schemes, which include a traditional extraction steam heating and a high- and low-side coupled heat-storage tank system. Since R2 and R3 have the same heat-release strategy, the boundaries of their electrothermal characteristic diagram are identical.

The maximum heating load of the traditional extraction steam (point B) increases from 271.28 MW to 377.52 MW in the coupled system (point H), and the heating load at point H is 35.49 % higher than that at point B.

At a constant heat load, the three coupling schemes lead to an improved electrical-load adjustment range. With traditional extraction steam heating, the adjustment range of the electrical load is 114.29 MW–300 MW. The minimum electrical load of the coupling system is reduced to 112.21 MW, while the R1 scheme boosts the electrical load to 312.81 MW and the R2 and R3 schemes increase the maximum electrical load to 323.43 MW. If the R2 and

R3 schemes are adopted, 211.21 MW can be provided for new energy. As the thermal load rises, the adjustment range of the electrical load falls. This is due to the higher amounts of steam pumped in the ternary molten-salt system leading to a reduction in the proportion of steam that can be used to regulate the work done by the low-pressure cylinder. Thus, the range of electrical-load regulation gradually decreases.

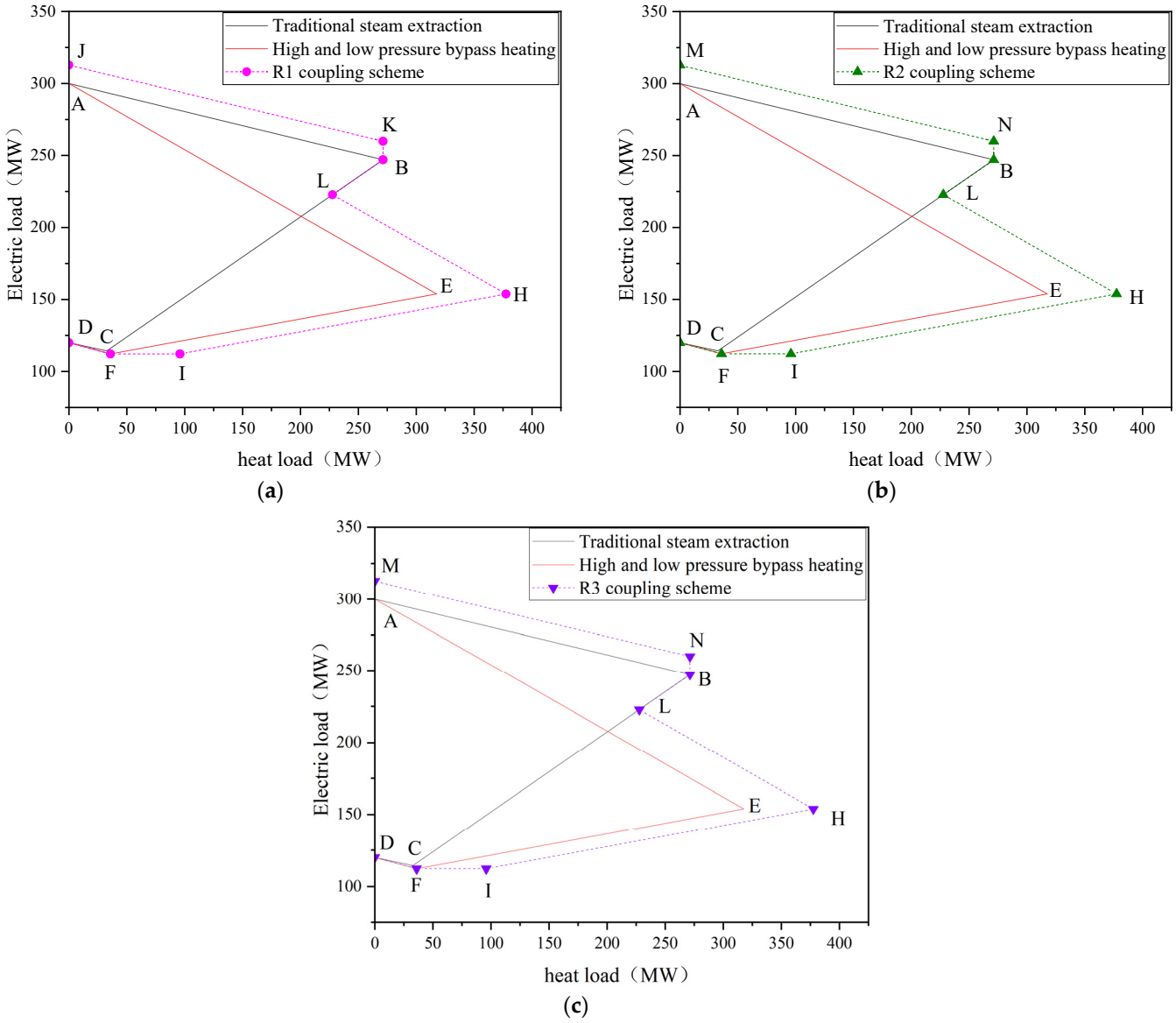

Figure 2. Electric heating characteristic diagram; (**a**) R1; (**b**) R2; (**c**) R3.

4.2. Maximum Thermoelectric Ratio

When the minimum cooling flow of the rated back pressure in the low-pressure cylinder is satisfied, the maximum thermoelectric ratios of the traditional extraction steam-heating system, high- and low-pressure bypass heating system, and the coupled systems vary according to the electrical load, as Figure 3 reveals.

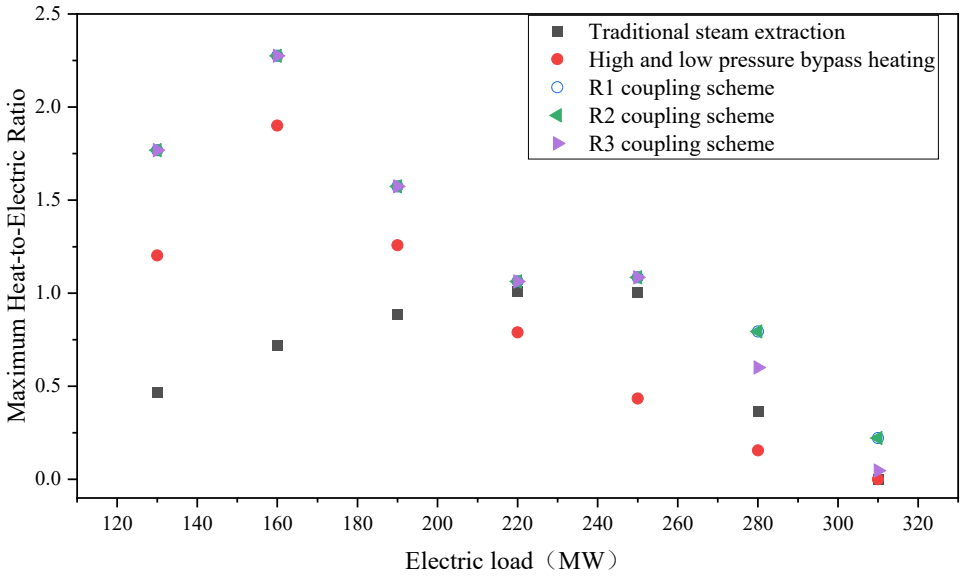

Figure 3. Maximum thermoelectric ratio comparison.

Figure 3 reveals that with an increase in electrical load, the maximum thermoelectric ratios of traditional extraction steam heating, high- and low-voltage bypass heating, and the coupled systems initially rise and then fall. This is due to an increase in the electric load allowing more steam to enter the steam turbine. As a result, the enthalpy value of the heat-extraction steam after work decreases and the heat-supply capacity falls. However, the export or import steam enthalpy value in the reheater of the coupled-system heating extraction system is higher than in the medium-pressure cylinder-extraction steam system or the heat-storage tank supplementary heating system, resulting in a greater heating capacity. When the electric load is steady, the maximum thermoelectric ratio of the coupled system is always greater than that of the traditional extraction steam-heating unit. Additionally, when the electric load is in the range of 130 MW–190 MW, the variations in the R1, R2, and R3 schemes are similar. This is because the output electric load is equivalent to the heat load affected by the heat-release power. When the electric load is 190 MW–310 MW, the output electric loads of the traditional extraction steam-heating system and the high- and low-pressure bypass heating system reaches 300 MW, while the maximum thermoelectric ratio approaches zero. Under a constant electric load, both the high- and low-pressure bypass heating system and the coupled system enhance the heating capacity of the unit, although the coupled system has a more considerable influence.

4.3. Minimum Charge Rate

When the unit is rated back pressure, Figure 4 presents the minimum charge rate of the traditional extraction steam-heating system, high- and low-pressure bypass heating system, and coupled systems, according to various heat loads.

Based on the relationship between the electrical-load output and the thermal-load output of the three coupling schemes illustrated in Figure 2, the minimum electrical-load output values for the three coupling schemes were observed to be closely similar when the thermal-load outputs ranged from 30 MW to 280 MW. Such findings are demonstrated by the similarity in the IH line. Despite similar trends, all three schemes were designed to decrease the minimum electrical-load factor and improve the peaking capacity of the unit. Thus, the minimum charge rate of the R1, R2, and R3 schemes is essentially the same. This is due to the minimum output load being constant and limited by the minimum cooling flow of the low-pressure cylinder and the regenerative extraction steam. When the heating load is 280 MW, the heating load for conventional extracted heat does not reach 280 MW, so the electrical-load output is zero for a heating load of 280 MW, and the minimum electrical load factor is, accordingly, zero. When the heat load is stable, the minimum charge rate of

the coupled system is less than that of the traditional extraction steam heating and high- and low-pressure bypass heating systems. The reason for this is the enthalpy value of the extraction steam in the coupled heating system is higher than that of the conventional medium-pressure cylinder. Under a stable heating load, the heat-storage tank supplements a part of the heat, resulting in lower steam extraction and more steam entering the turbine. Under the same heating load, the minimum charge rate of the coupled system is noticeably smaller, and the absorption capacity of new energy is better.

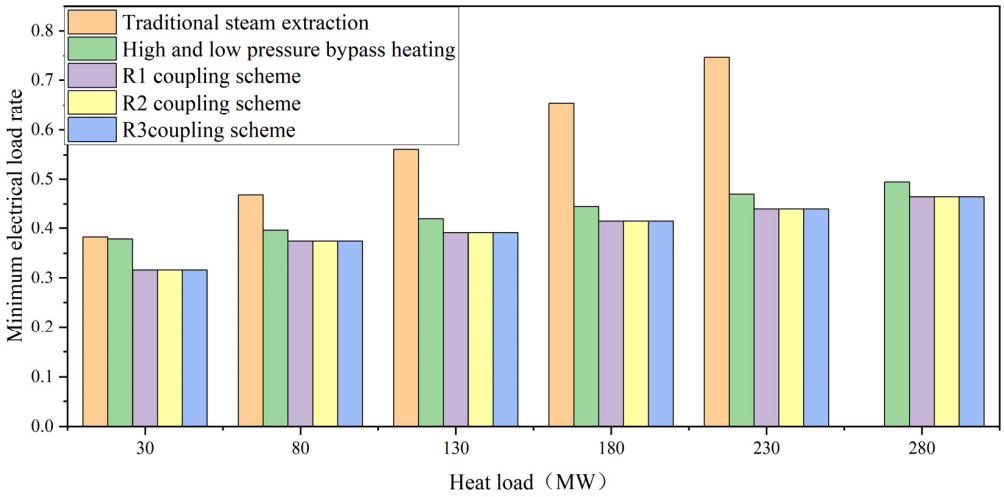

Figure 4. Comparison of the minimum charge rate.

4.4. Peak Regulating Capacity and Depth

When the high- and low-pressure side intake ratio is 4:6, the minimum cooling flow of the low-pressure cylinder at a back pressure of 3 kpa can be ensured in the unit under the premise of heat recovery and steam extraction. The newly added peak regulating capacity and peak regulating depth in the heat-storage processes of the three coupled schemes vary with the heat-storage load, as Figures 5 and 6 indicate.

The output load and new peak regulating capacity of the three coupling schemes are proportional to the heat-storage load. Figure 5a–c, respectively, represent the peak regulating capacity of R1, R2, and R3. As the heat-storage load increases, the output electrical load of the coupled system gradually falls, while the new peak regulating capacity progressively rises. This is due to steam being extracted for heat storage in the heat storage process under the 40% THA condition, thereby reducing the amount of steam entering the steam turbine. As Figure 6 reveals, increasing heat-storage loads leads to a steady rise in the peak regulating depth of the coupling system. When comparing the three coupling modes, the minimum output power of the coupling system in the R3 scheme is 54.45 MW, while the maximum peak regulating capacity is 65.55 MW. When the heat-storage load is 60 MW, the peak regulating depths of the R1, R2, and R3 schemes are 21.46%, 21.46%, and 21.85%, respectively. During the heat-storage process of R1 and R2, the molten salt is heated by the steam taken away from the reheater outlet, and the hydrophobic water, after heat exchange with the molten salt, enters the deaerator. When the heat storage load is 20 MW, 40 MW, and 60 MW, the influence on the electric-load output of the steam turbine is the same. The results suggest that the strategy of reheating-extracted cold steam as the heat source of the heat-storage tank is preferable to the reheating of extracted hot steam in the heat-storage process.

In the heat-release process, 40% of the heat stored under THA conditions is released. The outlet water supply of the feed pump is heated, and the heated steam is transported to LP1 to increase the working steam capacity of the low-pressure cylinder and the output electrical load of the unit, as Figures 7 and 8 show.

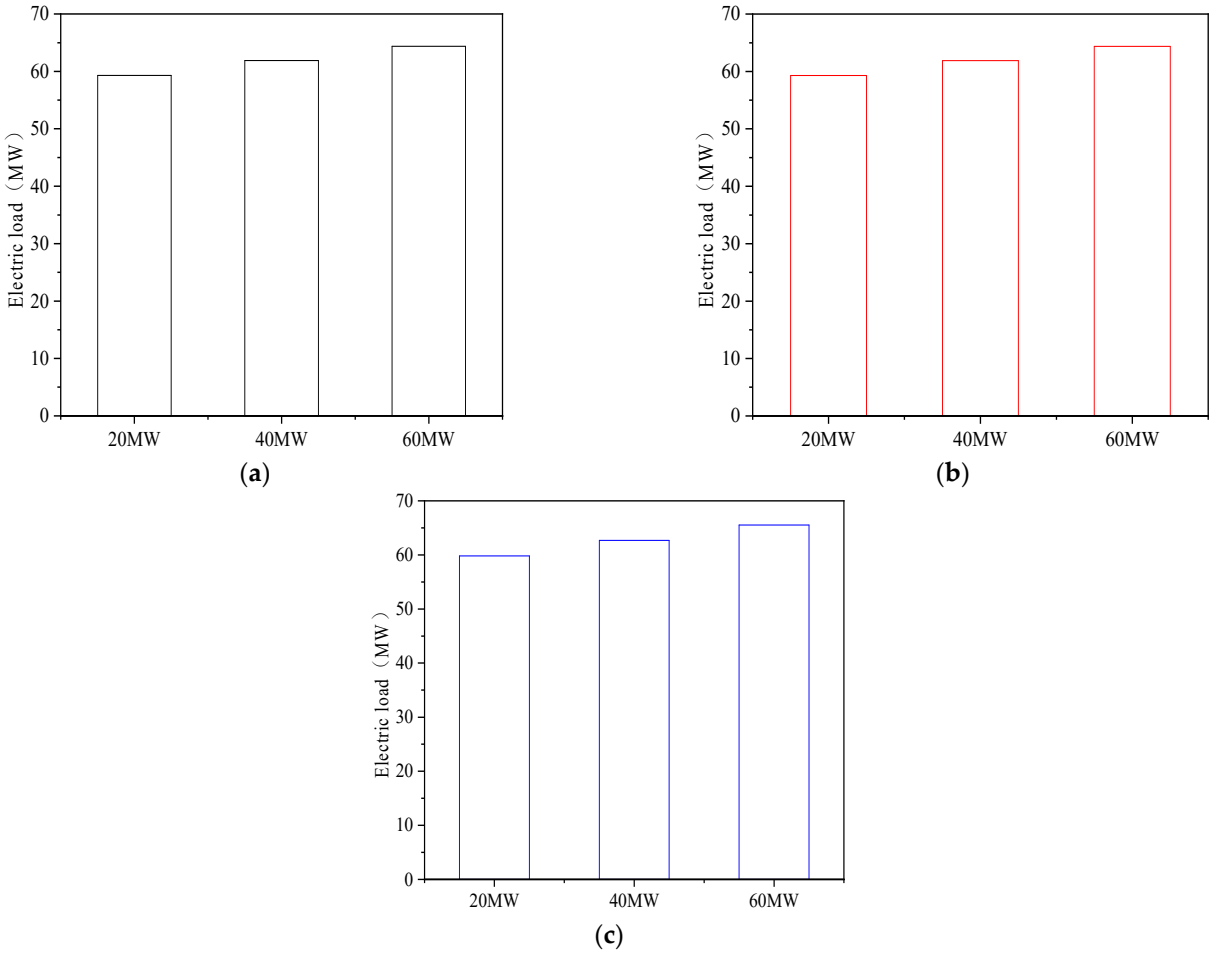

Figure 5. New peak regulating capacity of the heat-storage process coupling system. (**a**) R1; (**b**) R2; (**c**) R3.

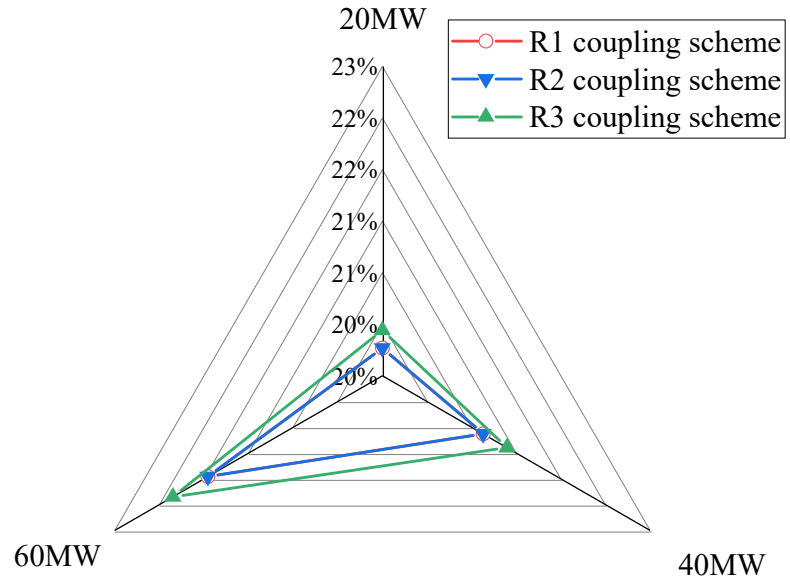

Figure 6. Peak regulating depth of the heat-storage process coupling system.

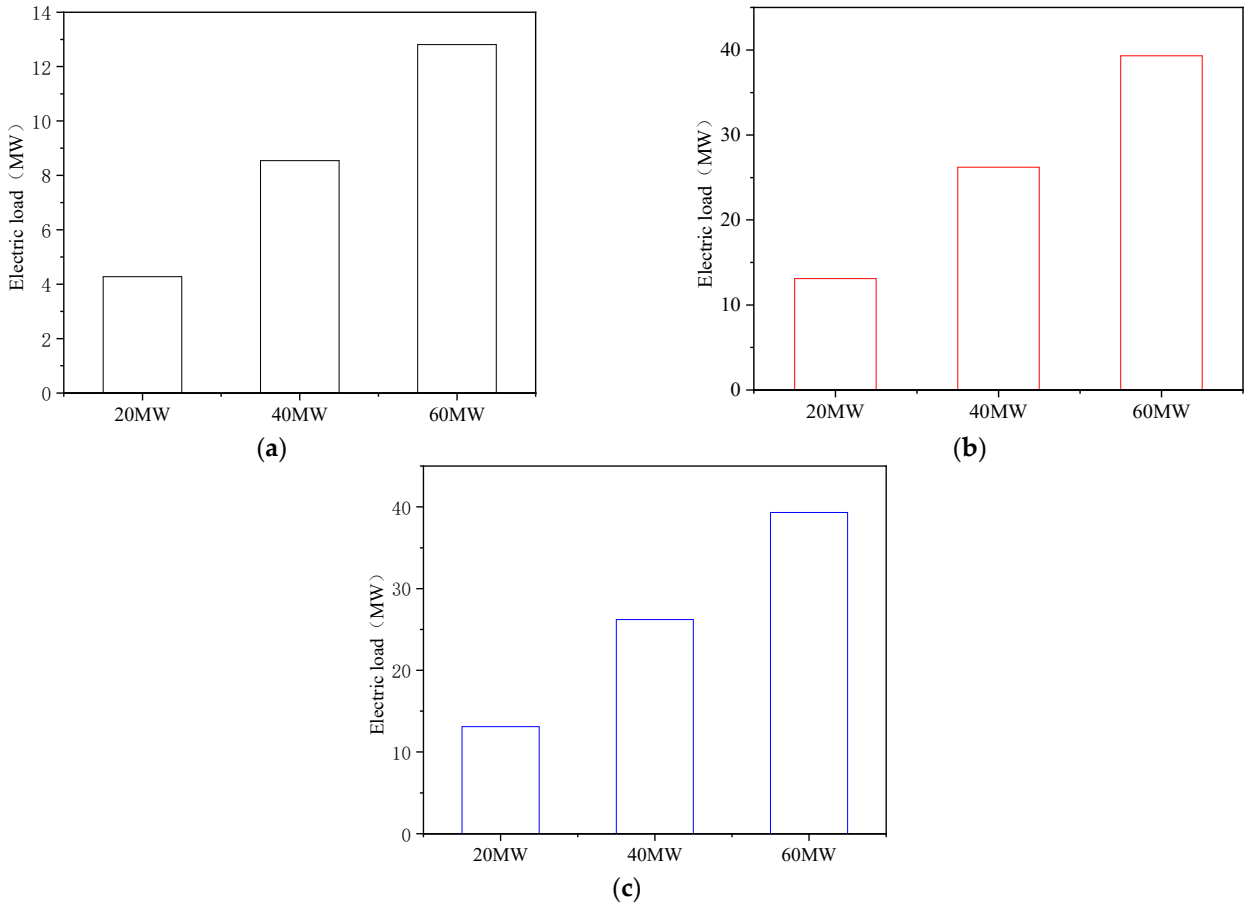

Figure 7. New peak regulating capacity of the coupled system in the heat-release process. (**a**) R1; (**b**) R2; (**c**) R3.

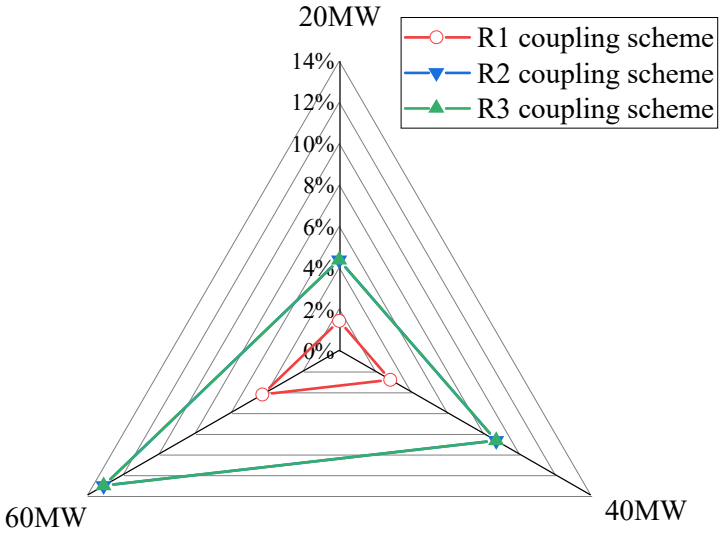

Figure 8. Peak regulating depth of the coupled system in the exothermic process.

Figure 7a–c, respectively, represent the peak regulating capacities of the R1, R2, and R3 coupling modes under different heat-release powers. The output electrical load, newly added peak regulating capacity, and peak regulating depth of the three coupling schemes are proportional to the heat-storage load. When the newly added peak regulating capacity and peak regulating depth of the three coupling schemes have the same heat-storage load,

the maximum output electrical loads of the R2 and R3 schemes are equal. During the heat-release process of R2 and R3, the molten salt is heated by the outlet water of the feed-water pump to reach the boiler inlet feed-water temperature, resulting in the reduction of heat pumping steam from the high-pressure cylinder and medium-pressure cylinder. When the heat-release load is 20 MW, 40 MW, and 60 MW, the influence on the electric-load output of the steam turbine is the same. When the heat-storage load is 60 MW, the maximum and minimum peak regulating capacities of the coupled system are 39.32 MW and 13.11 MW, respectively. Furthermore, the maximum and minimum peak regulating depths are 13.10% and 4.27%. The results suggest that due to the heat-release peak regulation effect, in the heat-release process, the strategy of using the outlet water of the feed pump as the water supply, after heating by the hot tank, is more desirable than directly sending the water to the low-pressure cylinder.

5. Conclusions

In this study, a 300 MW heating unit was used as a model and Aspen Plus software was employed to simulate and assess a traditional extraction steam-heating system, high- and low-pressure bypass heating system, and high- and low-pressure bypass heating system coupled to a heat-storage tank. The software was also applied to quantitatively analyse the safe-operating interval, maximum thermoelectric ratio, and minimum electric-load rate of the three systems. Furthermore, the peak regulating capacity and peak regulating depth of the unit at different heat storage loads were determined. The following conclusions were obtained:

(1) The high- and low-pressure bypass heating system and the coupling system can expand the safe operating range of the unit. The maximum heat load increased from 271.28 MW to 377.52 MW compared to traditional pump heating, which represents a relative increase of 35.49%. The R2 and R3 schemes increased the maximum electric load from 300 MW to 323.43 MW, which is a relative increase of 7.81%.

(2) When the generating load of the unit was 190 MW, the maximum thermoelectric ratio of the high- and low-pressure bypass heating system and coupling system increased from 0.89 to 1.26, signifying a 41.57% increase. When the heat load was 180 MW, the lowest electric load ratio of the high- and low-pressure bypass heating system and the coupling system fell by 32.31% from 0.65 to 0.44. Thus, the coupled heat storage arrangement of the high- and low-pressure bypass heating system improved the peak regulating capacity of the unit.

(3) By comparing the heat-storage peak regulation performance of the coupling schemes for three different heat-storage loads, the peak regulation capacity of the R3 scheme was better than the R1 and R2 schemes. The corresponding optimal heat storage load was 60 MW, the newly increased peak regulation capacity was 65.55 MW, and the newly increased peak regulation depth was 21.85%. A heat release peak regulating performance analysis revealed that the R2 and R3 schemes had better peak regulating capacity than the R1 scheme. These two schemes had a maximum heat-storage load of 60 MW, a newly added peak-regulating capacity of 39.32 MW, and a newly added peak-regulating depth of 13.10%.

Author Contributions: Conceptualization, H.Y., S.T. and M.H.; methodology, H.Y., S.T. and M.H.; software, H.Y.; writing—original draft preparation, H.Y. and M.H.; writing—review and editing, H.Y., S.T. and M.H. All authors have read and agreed to the published version of the manuscript.

Funding: This research was funded by the Basic Research Program of Shanxi Province (20210302123199), the Major Science and Technology Special Project of Shanxi Province (20201102006).

Institutional Review Board Statement: Not applicable.

Informed Consent Statement: No applicable.

Data Availability Statement: Data not available to be shared due to the technical limitations.

Conflicts of Interest: The authors declare no conflict of interest.

Nomenclature

D_{C0}	the exhaust flow rate of the low-pressure cylinder under THA conditions (t/h)
V_{c0}	rated exhaust steam specific capacity (m^3/kg)
V_{min}	minimum volume flow of the final stage
G_{v2min}	signifies the relative minimum volume flow of the final stage
G_{cmin}	minimum cooling flow of the low-pressure cylinder (t/h)
v_c	exhaust steam specific capacity of the low-pressure cylinder at different back pressures (m^3/kg)
x	thermoelectric ratio
P_e	output electrical load of the unit (MW)
Q_h	thermal load of the unit (MW)
λ	lowest charge rate
P_{e0}	output electrical load of the unit under rated working conditions (MW)
$\Delta P_{c,t}$	peak regulating capacity of storage process units (MW)
$\Delta P_{s,t}$	peak regulating capacity of heat release process units (MW)
$\Psi_{c,t}$	peak regulating depth of time t storage process units
$\Psi_{s,t}$	peak regulating depth of time t heat release units
$P_{c,t}$	output electrical load of the unit at time t of heat storage (MW)
$P_{s,t}$	output electrical load of the unit at time t of heat release (MW)
P_0	output electrical load of the unit under the 40% THA (MW)
THA	turbine heat acceptance

References

1. Fu, X.; Fan, W.; Lin, H.; Li, N.; Li, P.; Ju, L.; Zhou, F. A Risk Aversion Dispatching Optimal Model for a Micro Energy Grid Integrating Intermittent Renewable Energy and Considering Carbon Emissions and Demand Response. *Processes* **2019**, *7*, 916. [CrossRef]
2. Feng, S.; Zhang, X.; Zhang, H. Multi-objective optimization of coal-fired power units considering deep peaking regulation in China. *Environ. Sci. Pollut. Res.* **2022**, *30*, 10756–10774. [CrossRef]
3. Wei, Q.; Zheng, P.; Zou, S.; Bai, T. Research on the combined low pressure steam bypass and heat storage peak shaving for industrial extraction steam heating units. *Energy Rep.* **2021**, *8*, 179–187. [CrossRef]
4. Han, X.; Zhu, Q.; Guan, J.; Han, Z. Research on wet steam condensation flow characteristics of steam turbine last stage under zero output condition. *Int. J. Therm. Sci.* **2022**, *179*, 107691. [CrossRef]
5. Fu, H.; Fang, L.; Yu, M.; Cui, P.; Zhang, W.; Mao, Y.; Zhuang, Z.; Fang, Z. Influence and economic analysis of heat storage in the non-heating season on the heat extraction capacity of mid-deep borehole heat exchangers. *Energy Build.* **2023**, *278*, 112619. [CrossRef]
6. Xu, Z.; Gao, J.; Hu, B.; Wang, R. Multi-criterion comparison of compression and absorption heat pumps for ultra-low grade waste heat recovery. *Energy* **2021**, *238*, 121804. [CrossRef]
7. Manni, M.; Nicolini, A.; Cotana, F. Performance assessment of an electrode boiler for power-to-heat conversion in sustainable energy districts. *Energy Build.* **2022**, *277*, 112569. [CrossRef]
8. Chen, C.; Ge, Z.; Zhang, Y. Study of combined heat and power plant integration with thermal energy storage for operational flexibility. *Appl. Therm. Eng.* **2023**, *219*, 119537. [CrossRef]
9. Xue, Z.; Yang, R.; Wang, T.; Gu, W.; Gao, Q.; Zhang, Y. Application of turbine HP-LP bypass system combining with heating in supercritical 350 MW unit. *Therm. Power Gener.* **2018**, *47*, 101–105.
10. Wang, Z.; Cao, L.; Dong, E. Improving wind power accommodation of combined heat and power plant based on bypass system. *Acta Energ. Sol. Sin.* **2021**, *42*, 317–323.
11. Liu, M.; Wang, S.; Zhao, Y.; Tang, H.; Yan, J. Heat–power decoupling technologies for coal-fired CHP plants: Operation flexibility and thermodynamic performance. *Energy* **2019**, *188*, 116074. [CrossRef]
12. Wang, H.; Dong, X.; Yang, J. Study on Peak Shaving Range of Heat Storage Units Based on Aspen Plus. *Turbine Technol.* **2019**, *61*, 131–135.
13. Lai, F.; Wang, S.; Liu, M.; Yan, J. Operation optimization on the large-scale CHP station composed of multiple CHP units and a thermocline heat storage tank. *Energy Convers. Manag.* **2020**, *211*, 112767. [CrossRef]
14. Li, D.; Wang, J. Study of supercritical power plant integration with high temperature thermal energy storage for flexible operation. *J. Energy Storage* **2018**, *20*, 140–152. [CrossRef]
15. Trojan, M.; Taler, D.; Dzierwa, P.; Taler, J.; Kaczmarski, K.; Wrona, J. The use of pressure hot water storage tanks to improve the energy flexibility of the steam power unit. *Energy* **2019**, *173*, 926–936. [CrossRef]
16. Liu, C.; Geng, L.; Wand, H. Control strategy in transformation of high and low pressure bypass combined heat supply. *Therm. Power Gener.* **2020**, *49*, 126–132.
17. Wang, Z.; Cao, L.; Si, H. Analysis of electric output regulation capacity of low-pressure cylinder bypass heating of steam turbine. *Turbine Technol.* **2021**, *63*, 333–335.
18. Zhang, X.; Yujie, X.; Lijun, Y.; Lexuan, L.I.; Chen, H.; Zhou, X. Performance analysis and comparison of multi-type thermal power-heat storage coupling systems. *Energy Storage Sci. Technol.* **2021**, *10*, 1565.

19. Zhao, B.; Ding, J.; Wei, X.; Liu, B.; Lu, J.; Wang, W. Design and thermal stability study of $LiNO_3$-$NaNO_3$-KNO_3 ternary molten salt system. *CIESC J.* **2019**, *70*, 2083–2091.
20. Zaversky, F.; García-Barberena, J.; Sánchez, M.; Astrain, D. Transient molten salt two-tank thermal storage modeling for CSP performance simulations. *Sol. Energy* **2013**, *93*, 294–311. [CrossRef]
21. Lan, W.; Chen, G.; Zhu, X.; Wang, X.; Liu, C.; Xu, B. Biomass gasification-gas turbine combustion for power generation system model based on ASPEN PLUS. *Sci. Total Environ.* **2018**, *628–629*, 1278–1286. [CrossRef] [PubMed]
22. Li, Y.; Wang, N.; Guan, H.; Jia, Z.; Zhang, Y.; Zhao, G.; Gao, M. Optimization study of CO2 capture unit for subcritical coal-fired power generation unit based on Ebsilon and Aspen plus. *Energy Convers. Manag.* **2022**, *269*, 116111. [CrossRef]
23. Zhu, X.; Ma, H.; Han, Y. Comparison of thermoelectric decoupling modes of 300 MW subcritical unit. *Clean Coal Technol.* **2022**, *28*, 141–148.
24. Liu, J.; Ma, S.; Ma, H. Analysis on Thermal Peak Shaving and Economic Performance of Gas-Fired Unit. *Electr. Power* **2021**, *54*, 104–110.